Indonesian Journal of Cancer Chemoprevention, October 2025
ISSN: 2088–0197
e-ISSN: 2355-8989

UPLC-QToF-MS/MS–Based Metabolite Profiling and Network Pharmacology Analysis of Persimmon Vinegar Residue (*Diospyros kaki* L.) in Colorectal Cancer

Roihatul Mutiah*, Ermin Rachmawati, Ahmad Ulfi Baihaqi

Department of Pharmacy, Faculty of Medicine and Health Sciences, Maulana Malik Ibrahim State Islamic University, Malang, Indonesia

Abstract

Colorectal cancer is one of the most prevalent malignancies of the digestive tract, and currently available anticancer therapies are generally nonselective and may cause toxicity to normal cells. Persimmon (*Diospyros kaki* L.) is known to contain bioactive compounds with potential anticancer properties. However, residues generated during persimmon vinegar production are often discarded as waste despite retaining various metabolites with potential biological activities. This study aimed to characterize the metabolite profile and predict the molecular mechanisms underlying the anti-colorectal cancer potential of a 96% ethanol extract of persimmon vinegar residue using metabolomic and *in silico* approaches. UPLC-QToF-MS/MS analysis putatively identified 25 metabolites based on accurate mass measurements and database matching using MassLynx and ChemSpider, with major constituents including andrographolide, 1,2,3-propanetriol-ß-D-allopyranose (1:1), and 1,9-dideoxyforskolin. Network pharmacology analysis identified 40 overlapping target genes between the putatively annotated metabolites and colorectal cancer–related genes, which were enriched in several signaling pathways, including Wnt, MAPK, ErbB, PI3K/Akt, mTOR, apoptosis, and p53. These pathways were associated with 11 hub target genes, namely EGF, AKT1, JUN, MYC, MAPK1, MAPK3, BAX, CCND1, BCL2, TP53, and CASP3. Collectively, these findings provide preliminary evidence that persimmon vinegar residue contains bioactive metabolites associated with molecular targets and signaling pathways relevant to colorectal cancer, supporting its potential as a promising source of anti-colorectal cancer compounds that warrants further experimental validation.

Keywords: *persimmon vinegar,* Diospyros kaki *L., colorectal cancer, metabolite profiling, network pharmacology.*

Submitted: June 03, 2026
Revised: August 10, 2026
Accepted: August 21, 2026

*Corresponding author: roiha@farmasi.uin-malang.ac.id

INTRODUCTION

Colorectal cancer is one of the malignancies of the digestive tract with continuously increasing global prevalence and mortality, representing a significant health and economic burden, including in Indonesia (WHO, 2022; Bestari and Albanna, 2025). The risk of colorectal cancer is influenced by lifestyle and genetic factors; therefore, early screening plays an important role in reducing mortality associated with this disease (Puspitasari and Waluyo, 2021). To date, 5-fluorouracil–based chemotherapy remains the main therapeutic option, particularly in advanced stages; however, its nonselective nature results in various adverse effects due to damage to rapidly dividing normal cells, such as gastrointestinal disorders and peripheral neuropathy (Kemenkes, 2018). These limitations highlight the need for the development of anticancer agents that are more selective, effective, and safe, with clearly defined molecular mechanisms.

Persimmon (*Diospyros kaki* L.) is a plant belonging to the Ebenaceae family that is widely cultivated and known to be rich in bioactive compounds, such as flavonoids, tannins, phenolics, organic acids, and carotenoids, which play an important role as antioxidants (Kuncoro, *et al*., 2022). Various studies have shown that bioactive compounds in persimmon fruit possess anticancer potential through mechanisms including free radical scavenging, prevention of DNA damage, inhibition of cancer cell proliferation, and induction of apoptosis and cell cycle disruption, thus offering potential for development as preventive agents or adjuvant therapies for colorectal cancer (Bianchini, *et al*., 2024). Fermentation processes, which involve the activity of microorganisms in converting organic substrates into new products, have been widely utilized to enhance the functional value and bioactive metabolite content of food materials (Tarigan, 2017). One such fermented product is persimmon vinegar, which is rich in secondary metabolites; however, the solid residue generated from the fermentation process is often discarded as waste, despite still containing bioactive compounds with pharmacological value.

Persimmon vinegar residue has been reported to retain various bioactive constituents, including flavonoids, phenolic compounds, tannins, and organic acids, which exhibit antioxidant activity and may contribute to anti-cancer effects through the modulation of oxidative stress and carcinogenesis-related signaling pathways (Mutiah, *et al*., 2026). However, the metabolite composition of persimmon vinegar residue has not been comprehensively characterized, and its molecular mechanisms against colorectal cancer remain largely unexplored. Therefore, this study employed an integrated UPLC-QToF-MS/MS-based metabolomic approach combined with network pharmacology to comprehensively characterize the metabolite profile of persimmon vinegar residue and predict its potential molecular mechanisms against colorectal cancer. This integrated strategy provides a systematic framework for identifying bioactive metabolites and their associated molecular targets while supporting the valorization of persimmon vinegar residue as a potential source of natural product–based anticancer agents.

MATERIALS AND METHODS

Chemicals and Reagents

All chemicals were of analytical or UPLC grade. Ethanol 96% (technical grade) was obtained from a local supplier (Indonesia). Methanol (Hypergrade for UPLC), acetonitrile (Hypergrade for UPLC), and formic acid (ultrapure for UPLC) were purchased from Merck (Darmstadt, Germany). Ultrapure water containing 0.05% formic acid was used as the aqueous mobile phase.

Instruments

The instruments used in this study included a moisture content analyzer, an ultrasonic cleaner (Sonica, Italy), a rotary evaporator (Heidolph, Germany), and an ultra-performance liquid chromatography coupled with quadrupole time-of-flight tandem mass spectrometry system (UPLC-QToF-MS/MS; Waters, USA). UPLC-QToF-MS/MS analysis was conducted at the Forensic Laboratory Center, Indonesian National Police Criminal Investigation Agency (Puslabfor Bareskrim Polri), Sentul, Bogor, Indonesia.

Software and Databases

Chromatographic data acquisition and interpretation were performed using MassLynx version 4.1 (Waters, USA), while compound identification was assisted by the ChemSpider database (https://www.chemspider.com). Prediction of physicochemical properties was conducted usingpkCSM(https://biosig.unimelb.edu.au/pkcsm/prediction), toxicity prediction using ProTox-II (http://tox.charite.de/), and bioactivity prediction using PASS Online (https://way2drug.com/PassOnline). Network pharmacology analysis employed GeneCards (https://www.genecards.org) to obtain target genes, DisGeNET (https://www.disgenet.org) for disease-associated genes, STRING (https://www.string-db.org) for protein–protein interaction analysis, Cytoscape version 3.10.1 (https://cytoscape.org) for network visualization, and Kyoto Encyclopedia of Genes and Genomes (KEGG) PATHWAY database (https://www.genome.jp/kegg/pathway.html) for pathway enrichment analysis.

Sample Preparation

Fresh young persimmon fruits (D*iospyros kaki* L.) weighing approximately 150 kg were selected, washed thoroughly under running water, drained, and cut into small pieces. The fruits were subjected to spontaneous fermentation without the addition of microbial starter cultures by allowing the persimmon juice to ferment naturally at room temperature in tightly sealed containers for six months, following the method described by Febriani and Azizati (2018). After the six-month fermentation period, the fermented product was allowed to cool to room temperature before subsequent processing.

The solid residue obtained after fermentation was washed with running water and dried in a drying chamber for approximately 48 h until a constant weight was achieved. The dried residue was then pulverized using a grinding machine to obtain a fine powder. The persimmon vinegar residue powder was stored in airtight containers containing silica gel to control moisture and kept in a dedicated herbal material storage cabinet until further analysis.

Extraction

Prior to extraction, the moisture content of persimmon vinegar residue powder (*Diospyros kaki* L.) was measured. The powder was extracted with 96% ethanol (1:10, w/v) using ultrasonic-assisted extraction for 30 min, filtered, and concentrated under reduced pressure. The resulting extract was oven-dried to a paste-like consistency, weighed (~10 mg), and stored for subsequent analysis.

Metabolite Profiling by UPLC-QToF-MS/MS

Accurately weighed extract (10.0 mg) was dissolved in methanol and diluted to 10 mL in a volumetric flask. The solution was filtered through a 0.2 µm syringe filter, and a 5 µL aliquot was injected into the UPLC system for analysis, with each sample analyzed in four replicates. Chromatographic separation was performed on an ACQUITY UPLC BEH C18 column (2.1 × 100 mm, 1.7 µm; Waters, Milford, MA, USA) maintained at 50°C using a gradient elution system consisting of mobile phase A (water containing 5 mM ammonium formate) and mobile phase B (acetonitrile containing 0.05% formic acid) at a flow rate of 0.2 mL min^{-1}. Mass spectrometric analysis was

performed exclusively in positive electrospray ionization (ESI+) mode because positive ionization generally provides higher ionization efficiency and sensitivity for a broader range of compounds analyzed by LC-MS, generating more abundant protonated molecular ions ($[M+H]^+$) that facilitate metabolite annotation based on accurate mass and MS/MS fragmentation patterns (Liigand, *et al.*, 2017). Mass spectra were acquired over an m/z range of 50–1300 using a Xevo G2-S QToF mass spectrometer (Waters, Milford, MA, USA). The source temperature and desolvation temperature were set at 100°C and 350°C, respectively, with a desolvation gas flow of 793 L h^{-1} and cone gas flow of 0 L h^{-1}. Collision energy was set at 4 V for low-energy acquisition and ramped from 25 to 70 V for high-energy acquisition. The chromatographic and mass spectrometric conditions followed the validated analytical method routinely employed by the analytical laboratory for untargeted metabolomic analysis.

Chromatographic and mass spectral data were processed using MassLynx software. The confidence of putative compound annotation was evaluated using the FitConf (%) value generated by the MassLynx elemental composition tool. Putative compound annotation was performed by matching accurate mass, elemental composition, and MS/MS fragmentation patterns with entries in the ChemSpider database.

Prediction of Physicochemical Properties and Toxicity

Physicochemical properties of the identified compounds were predicted using the pkCSM platform based on SMILES notation, applying Lipinski's rule of five parameters, including molecular weight, Log*P*, hydrogen bond donors and acceptors, topological polar surface area, and rotatable bonds. Compounds fulfilling Lipinski's criteria were further subjected to toxicity prediction using the ProTox-II database, with compounds classified as toxicity class ≥3 (LD_{50}) considered acceptable.

Bioactivity Prediction

Bioactivity prediction was performed for compounds that met physicochemical and toxicity criteria using PASS Online. Compounds with a probability of activity (Pa) >0.5 were selected, focusing on antineoplastic, chemopreventive, apoptosis agonist, and colon cancer–related activities.

Network Pharmacology Test

Target genes of compounds identified by UPLC-QToF-MS/MS and colorectal cancer–related genes were collected from GeneCards and DisGeNET. Overlapping targets were identified using a Venn diagram and were used to construct a compound–target network using Cytoscape v3.10.1, in which nodes represent compounds and proteins and edges indicate interactions. Targets with high degree connectivity were defined as key targets.

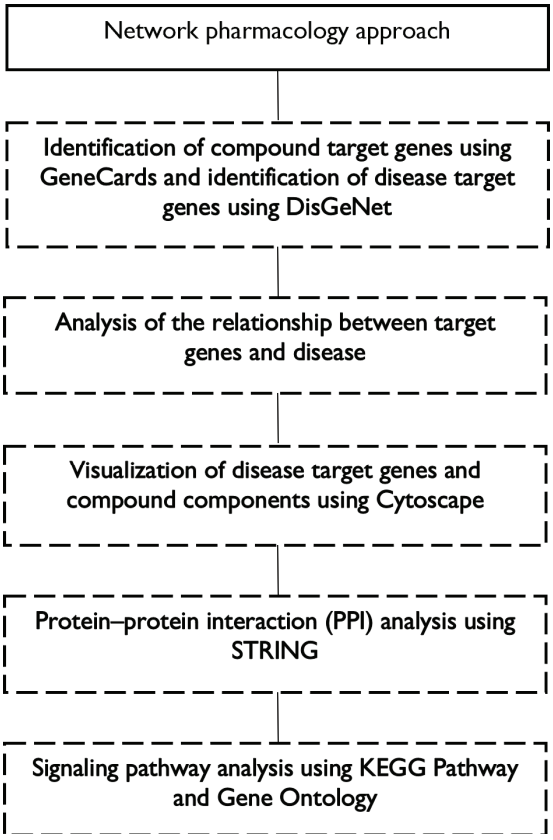


Figure 1. Network pharmacology test flow.

Protein–protein interaction (PPI) analysis was performed using STRING with a minimum confidence score of 0.400, followed by Gene Ontology and KEGG pathway enrichment analyses to identify the major biological pathways involved in colorectal cancer.

RESULTS

Metabolite Profile of Persimmon Vinegar Residue Based on UPLC-QToF-MS/MS

The metabolite profile of persimmon vinegar residue extract (*Diospyros kaki* L.) was analyzed using UPLC-QToF-MS/MS, which enables sensitive and accurate identification of compounds from complex matrices. Raw chromatographic and mass spectral data were processed using MassLynx software, in which detected ions were evaluated based on retention time, accurate mass, and signal quality prior to compound annotation using the ChemSpider database. This approach is effective in reducing matrix interference and enhancing metabolite signal clarity, thereby supporting comprehensive characterization of bioactive compounds (Dalimunthe, 2021). Compound separation on a C18 column showed a distribution of metabolites with varying degrees of polarity, in which highly polar compounds were detected earlier than more hydrophobic compounds, consistent with the characteristics of the nonpolar stationary phase and the gradient elution system employed (Hakim, *et al*., 2018).

Mass spectrometric analysis in positive ESI mode generated protonated molecular ions $[M+H]^+$ with high resolution, enabling accurate determination of molecular masses. MS/MS fragmentation produced characteristic diagnostic ion patterns for each compound, which played an important role in confirming molecular structures (Lei, *et al*., 2023). The use of a high-resolution UPLC system contributed to sharp separation and efficient analysis time, as reported in previous metabolomic studies (Lestari, *et al*., 2024). The resulting chromatographic profile (Figure 2) showed the presence of multiple peaks with varying intensities, reflecting the complexity of the metabolite composition of persimmon vinegar residue.

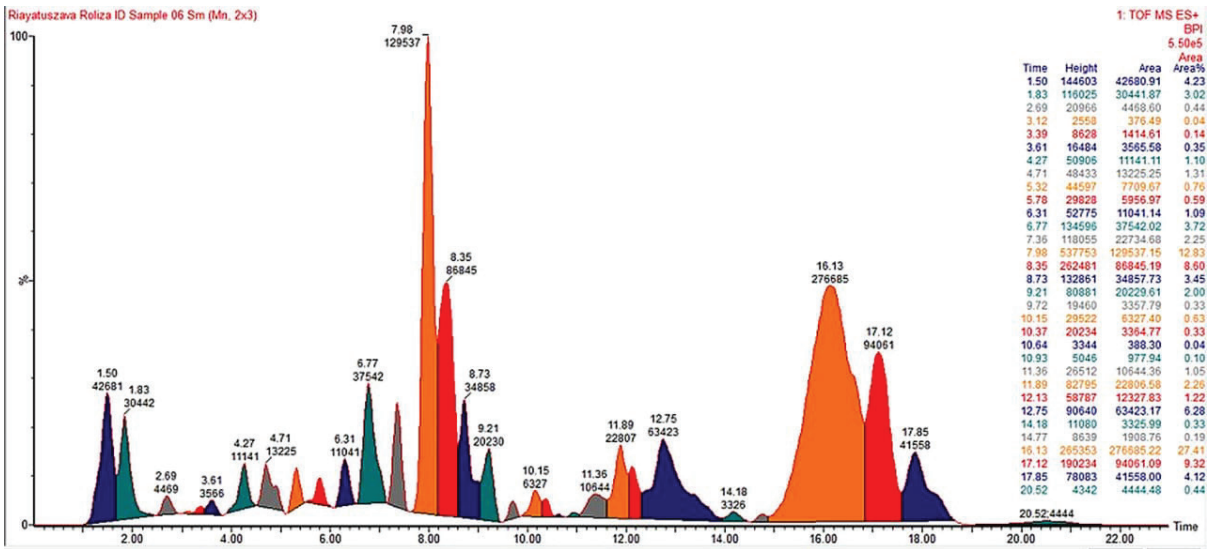


Figure 2. Base Peak Ion (BPI) chromatogram of the 96% ethanol extract of persimmon vinegar residue obtained by UPLC-QToF-MS/MS analysis.

Table 1. Metabolite profile of *Diospyros kaki* L. vinegar residue.

No	RT	%Area	*Measured Mass*	*Calculated Mass*	Molecular Formula	Compound Name
1	1.50	4.23	381.0800	381.0822	C17H16O10	CHEMBL479499
2	1.83	3.02	189.0769	189.0736	C4H8N6O3	bis(carbamoylamino)methyliden eurea
3	2.69	0.44	180.0671	180.0634	C5H5N7O	8-nitroso-[1,2,4]triazolo[1,5-c]pyrimidine-5,7-diamine
4	3.12	0.04	230.1029	230.1028	C10H15NO5	1,2-Pyrrolidinedicarboxylic acid, 5-oxo-, 1-(1,1-dimethylethyl) ester, (2S)-
5	3.39	0.14	231.0877	231.0869	C10H14O6	Methacryloyloxyethyl succinate
6	3.61	0.35	294.1556	294.1553	C12H23NO7	N-Fructosyl isoleucine
7	4.27	1.10	358.1718	358.1713	C13H27NO10	CHEMBL1277063
8	4.71	1.31	158.0826	158.0790	C3H7N7O	2-(5-Amino-1H-tetrazol-1-yl)acetohydrazide
9	5.32	0.76	195.1140	195.1093	C5H14N4O4	2-Ethyl-2-{[ethyl(nitro)amino]methyl}-1-hydroxyhydrazine 1-oxide
10	5.78	0.59	158.0824	158.0790	C3H7N7O	2-(5-aminotetrazol-1-yl)acetohydrazide
11	6.31	1.09	210.1138	210.1103	C7H11N7O	2-[5-(1H-Tetrazol-1-ylmethyl)-1,3,4-oxadiazol-2-yl]-2-propanamine
12	6.77	3.72	231.1143	2311107	C9H10N8	5-Amino-1-(6-hydrazino-3-pyridazinyl)-3-methyl-1H-pyrazole-4-carbonitrile
13	7.36	2.25	229.0992	2290995	C12H17O2Cl	Fenpentadiol
14	7.98	12.83	183.0926	1830922	C12H10N2	Harmane
15	8.35	8.60	227.0829	2270794	C9H6N8	9-Methylbistetrazolo[1,5-a:5′,1′-c]quinoxaline
16	8.73	3.45	211.1456	211.1420	C7H14N8	N-[3-(4H-1,2,4-Triazol-3-yl)propyl]imidodicarbonimidic diamide
17	10.15	0.63	273.1137	273.1186	C9H20O9	1,2,3-Propanetriol - β-D-allopyranose (1:1)
18	10.37	0.33	273.1135	273.1127	C16H16O4	p-Anisoin
19	10.93	0.10	383.2048	383.2070	C20H30O7	T-2 triol
20	11.36	1.05	367.2102	367.2121	C20H30O6	Dibutoxyethylphthalate
21	11.89	2.26	181.1234	181.1202	C7H12N6	6-(1-Pyrrolidinyl)-1,3,5-triazine-2,4-diamine
22	12.75	6.28	351.2148	351.2171	C20H30O5	Andrographolide
23	14.18	0.33	379.2452	379.2484	C22H34O5	1,9-dideoxyforskolin
24	14.77	0.19	316.2847	316.2825	C14H33N7O	N-{4-[(4-Aminobutyl)amino]butyl}-N~5~-(diaminomethylene)-L-ornithinamide
25	20.52	0.44	203.0541	203.0556	C8H10O6	cis-Dihomoaconitic acid

Peak alignment was not performed because the present study focused on metabolite characterization of a single extract rather than comparative metabolomic analysis across different sample groups.

Compound annotation was performed based on the chromatographic and mass spectral data, and the resulting annotations are presented in Table 1. The reported metabolites should be regarded as putatively annotated compounds based on accurate mass measurements and ChemSpider database matching, as no authentic reference standards were used for structural confirmation.

Among the annotated metabolites, harmane was the major compound, accounting for 12.83% of the total peak area, with a FitConf value of 92.3%. Other compounds with relatively high peak areas included 9-Methylbistetrazolo[1,5-a:5′,1′-c]quinoxaline (8.60%) and andrographolide (6.28%). Other compounds detected included 1,2,3-propanetriol–β-D-allopyranose (1:1), 1,9-dideoxyforskolin, and cis-dihomoaconitic acid.

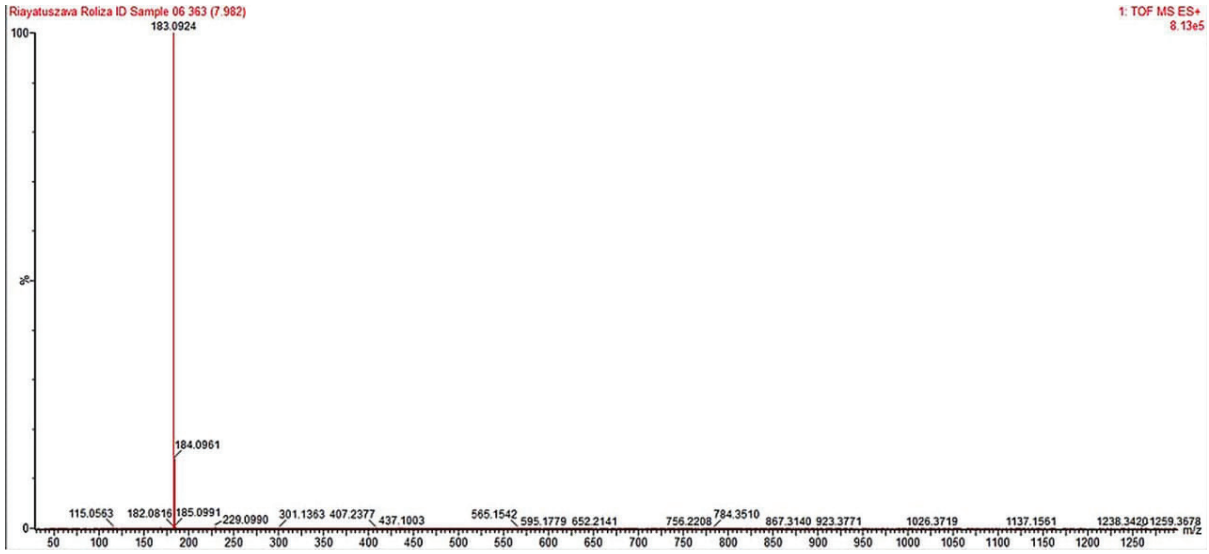


Figure 3. Spectra and chemical structures of major compounds in persimmon vinegar residue.

Harmane was detected at a retention time of 7.98 min, with a measured mass of 183.0926 and a calculated mass of 183.0922 for the molecular formula C12H10N2. Andrographolide was detected at a retention time of 12.75 min, with a measured mass of 351.2148 and a calculated mass of 351.2171 for C20H30O5. 1,9-Dideoxyforskolin was detected at a retention time of 14.18 min, with a measured mass of 379.2452 and a calculated mass of 379.2484 for C22H34O5.

Predicted Physicochemical Properties and Toxicity

The predicted physicochemical properties of the annotated compounds are presented in Table 2. Based on Lipinski's Rule of Five, 22 compounds met the predefined criteria, whereas three compounds did not. The evaluated parameters included molecular weight, log P, hydrogen bond acceptors (HBA), hydrogen bond donors (HBD), torsional bonds, and polar surface area (PSA).

Table 2. Predicted physicochemical properties of compounds from *Diospyros kaki* L. vinegar residue.

No	Compound Name	Lipinski's Rule of Five Parameters						Remark
		BM (g/mol)	Log *P*	HBA	HBD	Torsion	PSA (Å²)	
1	CHEMBL479499	380.305	-0.5765	10	5	3	149.937	Acceptable
2	CID: 253189	188.147	-2.2423	3	5	0	72.333	Acceptable
3	CID: 4656648	179.143	-0.3134	8	2	1	71.551	Acceptable
4	CID: 104412	229.232	0.9971	4	1	1	93.170	Acceptable
5	Methacryloyloxyethyl succinate	230.216	0.5137	5	1	7	92.840	Acceptable
6	CID: 139292115	293.316	-2.1232	7	6	7	116.544	Acceptable
7	CHEMBL1277063	357.356	-6.4576	11	10	8	137.815	Unacceptable
8	CID: 16765167	157.137	-2.7548	7	3	2	61.506	Acceptable
9	ChemSpider ID:9804503	194.191	-1.5337	5	2	6	75.568	Acceptable
10	CID: 16765167	157.137	-2.7548	7	3	2	61.506	Acceptable
11	ChemSpider ID:27799642	209.213	-0.7018	8	1	3	85.474	Acceptable
12	CID: 6410564	230.235	-0.2898	8	3	2	96.826	Acceptable
13	Fenpentadiol	228.719	2.7085	2	2	3	95.513	Acceptable
14	Harmane	182.226	3.0245	1	1	0	81.588	Acceptable
15	CID: 1229629	226.203	-0.0732	8	0	0	94.872	Acceptable
16	ChemSpider ID:45087548	210.245	-1.2553	4	6	4	86.683	Acceptable
17	ChemSpider ID:2341169	272.250	-4.8895	9	8	3	103.126	Acceptable
18	p-Anisoin	272.300	2.6201	4	1	5	117.131	Acceptable
19	T-2 triol	382.453	0.5511	7	3	4	158.845	Acceptable
20	Dibutoxyethylphthalate	366.454	3.6336	6	0	14	155.318	Unacceptable
21	CID: 200843	180.215	-0.3638	6	2	1	75.984	Acceptable
22	Andrographolide	350.455	1.9626	5	3	3	148.934	Acceptable
23	CID: 107948	378.509	3.4342	5	1	2	162.040	Acceptable
24	ChemSpider ID:9100353	315.466	-1.4078	5	6	14	133.000	Unacceptable
25	CID: 25244890	202.162	0.3369	3	3	6	79.472	Acceptable

The three compounds classified as unacceptable based on the evaluated criteria were CHEMBL1277063, dibutoxyethylphthalate, and ChemSpider ID:9100353. The remaining 22 compounds were classified as acceptable according to the predefined physicochemical criteria.

Compounds that met Lipinski's Rule of Five were subsequently subjected to toxicity prediction using the ProTox-II online platform. Toxicity prediction was performed by inputting the SMILES code of each compound. The predicted LD_{50} values and toxicity classes are presented in Table 3. Of the evaluated compounds, 21 met the predefined toxicity criterion, whereas one compound did not.

Table 3. Predicted toxicity results of compounds from *Diospyros kaki* L. vinegar residue.

No	Compound Name	LD_{50}	Toxicity Class	Remark
1	CHEMBL479499	5000	5	Acceptable
2	CID: 253189	1750	4	Acceptable
3	CID: 4656648	900	4	Acceptable
4	CID: 104412	1600	4	Acceptable
5	Methacryloyloxyethyl succinate	3300	5	Acceptable
6	CID: 139292115	5000	5	Acceptable
7	CID: 16765167	3000	5	Acceptable
8	ChemSpider ID:9804503	550	4	Acceptable
9	CID: 16765167	3000	5	Acceptable
10	ChemSpider ID:27799642	500	4	Acceptable
11	CID: 6410564	200	3	Acceptable
12	Fenpentadiol	940	4	Acceptable
13	Harmane	1000	4	Acceptable
14	CID: 1229629	300	3	Acceptable
15	ChemSpider ID:45087548	300	3	Acceptable
16	ChemSpider ID:2341169	23000	6	Acceptable
17	p-Anisoin	3000	5	Acceptable
18	T-2 triol	4	1	Unacceptable
19	CID: 200843	2000	4	Acceptable
20	Andrographolide	1890	4	Acceptable
21	CID: 107948	2550	5	Acceptable
22	CID: 25244890	700	4	Acceptable

The compound T-2 triol was classified as unacceptable, with a predicted LD_{50} value of 4 mg/kg and toxicity class 1. The other evaluated compounds were classified as acceptable, with toxicity classes ranging from 3 to 6.

Bioactivity Prediction

Bioactivity prediction was performed using PASS Online by inputting the SMILES codes of the compounds. Biological activities were selected based on probability of activity (Pa) values greater than 0.5. The predicted activities included antineoplastic, apoptosis agonist, chemopreventive, and antineoplastic activity specific to colorectal cancer.

Eight compounds exhibited predicted biological activities with Pa values greater than 0.5. These compounds were CHEMBL479499, 8-nitroso-[1,2,4]triazolo[1,5-c]pyrimidine-5,7-diamine (CID: 4656648), 1,2-pyrrolidinedicarboxylic acid, 5-oxo-, 1-(1,1-dimethylethyl) ester, (2S)-, methacryloyloxyethyl succinate, 1,2,3-propanetriol–β-D-allopyranose (1:1), andrographolide, 1,9-dideoxyforskolin, and cis-dihomoaconitic acid. The predicted biological activities comprised antineoplastic effects, apoptosis agonistic activity, and chemopreventive properties. Andrographolide showed the highest predicted Pa value for antineoplastic activity (Pa=0.949), followed by apoptosis

Table 4. Predicted bioactivity results of compounds using PASS online.

No	Compound Name	Pa	Biological Activity
1	CHEMBL479499	0.786	Antineoplastic
		0.898	Chemopreventive
		0.660	Apoptosis Agonist
2	8-nitroso-[1,2,4]triazolo[1,5-c]pyrimidine-5,7-diamine	0.531	Antineoplastic
3	1,2-Pyrrolidinedicarboxylic acid, 5-oxo-, 1-(1,1-dimethylethyl) ester, (2S)-	0.526	Apoptosis Agonist
4	Methacryloyloxyethyl succinate	0.526	Apoptosis Agonist
5	1,2,3-Propanetriol - β-D-allopyranose (1:1)	0.833	Antineoplastic
		0.573	Chemopreventive
		0.660	Apoptosis Agonist
6	Andrographolide	0.949	Antineoplastic
		0.538	Antineoplastic (colon cancer)
		0.640	Chemopreventive
		0.909	Apoptosis Agonist
7	1,9-dideoxyforskolin	0.667	Antineoplastic
		0.624	Chemopreventive
		0.567	Apoptosis Agonist
8	cis-Dihomoaconitic acid	0.692	Apoptosis Agonist

agonist activity (Pa=0.909), chemopreventive activity (Pa=0.640), and antineoplastic activity specific to colon cancer (Pa=0.538). CHEMBL479499 showed Pa values of 0.786 for antineoplastic activity, 0.898 for chemopreventive activity, and 0.660 for apoptosis agonist activity. 1,2,3-Propanetriol–β-D-allopyranose (1:1) showed Pa values of 0.833 for antineoplastic activity, 0.573 for chemopreventive activity, and 0.660 for apoptosis agonist activity. Meanwhile, 1,9-dideoxyforskolin showed Pa values of 0.667, 0.624, and 0.567 for antineoplastic, chemopreventive, and apoptosis agonist activities, respectively.

Table 5. Target protein screening results.

No	Compound Name	Number of Target Genes	Gifts Range	Relavance Score Range
1	Methacryloyloxyethyl succinate	4	20-61	1.45-4.69
2	1,2,3-Propanetriol - β-D-allopyranose (1:1)	436	10-68	0.34-47.79
3	Andrographolide	81	8-67	0.22-4.69
4	1,9-dideoxyforskolin	26	2-65	0.43-5.32

Indonesian Journal of Cancer Chemoprevention, October 2025
ISSN: 2088–0197
e-ISSN: 2355-8989

Network Pharmacology Analysis

Network pharmacology analysis was conducted to identify potential target proteins and biological pathways associated with the compounds of interest and colorectal cancer.

Target Protein Screening

Target proteins associated with the compounds were screened using the GeneCards database. A total of 547 target proteins associated with the evaluated compounds were identified.

The four compounds included in the target screening were methacryloyloxyethyl succinate, 1,2,3-propanetriol–β-D-allopyranose (1:1), andrographolide, and 1,9-dideoxyforskolin. The respective numbers of target genes were 4, 436, 81, and 26.

Disease-Related Target Screening

Of the 547 compound-related target proteins, 40 overlapped with 162 proteins associated with colorectal cancer obtained from the DisGeNET database. These 40 overlapping proteins were subsequently considered colorectal cancer-related target proteins in the network pharmacology analysis.

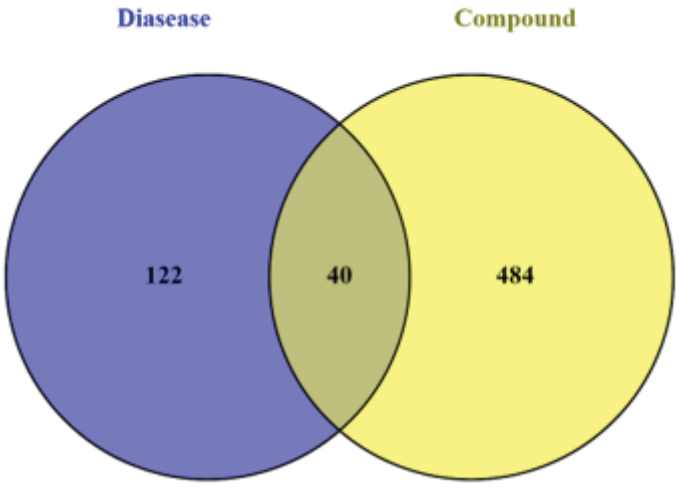


Figure 4. Venn diagram showing the overlap between colorectal cancer-associated target genes and target genes of compounds from *Diospyros kaki* L. vinegar residue.

Based on the Venn diagram, the yellow region represents the 547 target genes derived from persimmon vinegar residue, whereas the blue region represents the 162 target genes related to colorectal cancer. The 40 genes located in the overlapping region represent the common targets between the compounds and colorectal cancer.

The target network was subsequently visualized using Cytoscape, as shown in Figure 5. A total of 40 target proteins were identified, namely CEACAM5,NFKB1,TIMP1,AKT1,TP53,VEGFA, TYMS, HPGD, KDR, BAX, STAT3, IL6, PIK3CG, TNF, DKK1, B2M, BCL2, NFE2L2, IL1B, MMP9, MAPK1, EGF, MYC, CCND1, GAST, JUN, MAPK3, IFNG, MKI67, ICAM1, SRC, MAPK14, CASP3, ADA, KCNQ1, LGALS3, CEL, IL1RN, IGF1R, and INS.

Three bioactive components were associated with these target proteins, namely andrographolide, 1,2,3-propanetriol–β-D-allopyranose (1:1), and 1,9-dideoxyforskolin.

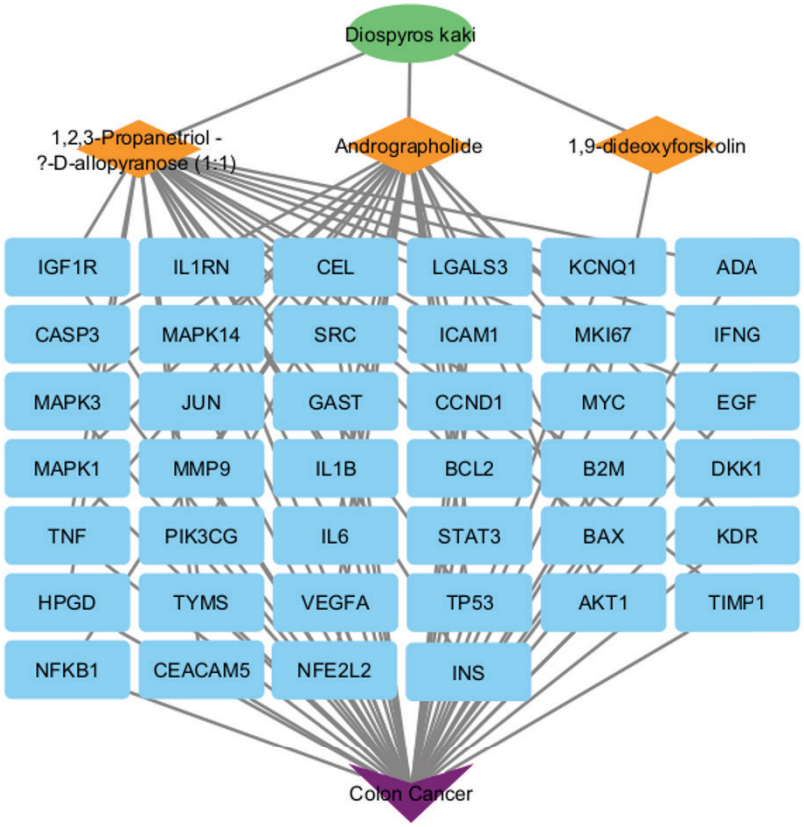


Figure 5. Network visualization of *Diospyros kaki* L. vinegar residue (green: plant name; orange: bioactive compounds; blue: target proteins; purple: disease).

Protein-Protein Interaction and Gene Ontology Enrichment Analysis

Protein–protein interaction analysis was performed using the STRING database. The resulting network consisted of 40 nodes and 436 edges, with a PPI enrichment p-value of $<1.0 \times 10^{-16}$.

Gene Ontology enrichment analysis was performed to evaluate the biological processes, molecular functions, and cellular components associated with the target proteins. The enrichment bubble plot identified 10 biological processes with high enrichment potential. Negative regulation of apoptotic processes exhibited the highest significance and involved 31 genes. Other enriched biological processes involved 27–31 associated genes, as shown in Figure 6B.

The molecular functions with the highest enrichment potential are presented in Figure 6C, whereas the cellular components with the highest enrichment potential are presented in Figure 6D. The most significantly enriched cellular components were vesicle-related components.

Indonesian Journal of Cancer Chemoprevention, October 2025
ISSN: 2088–0197
e-ISSN: 2355-8989

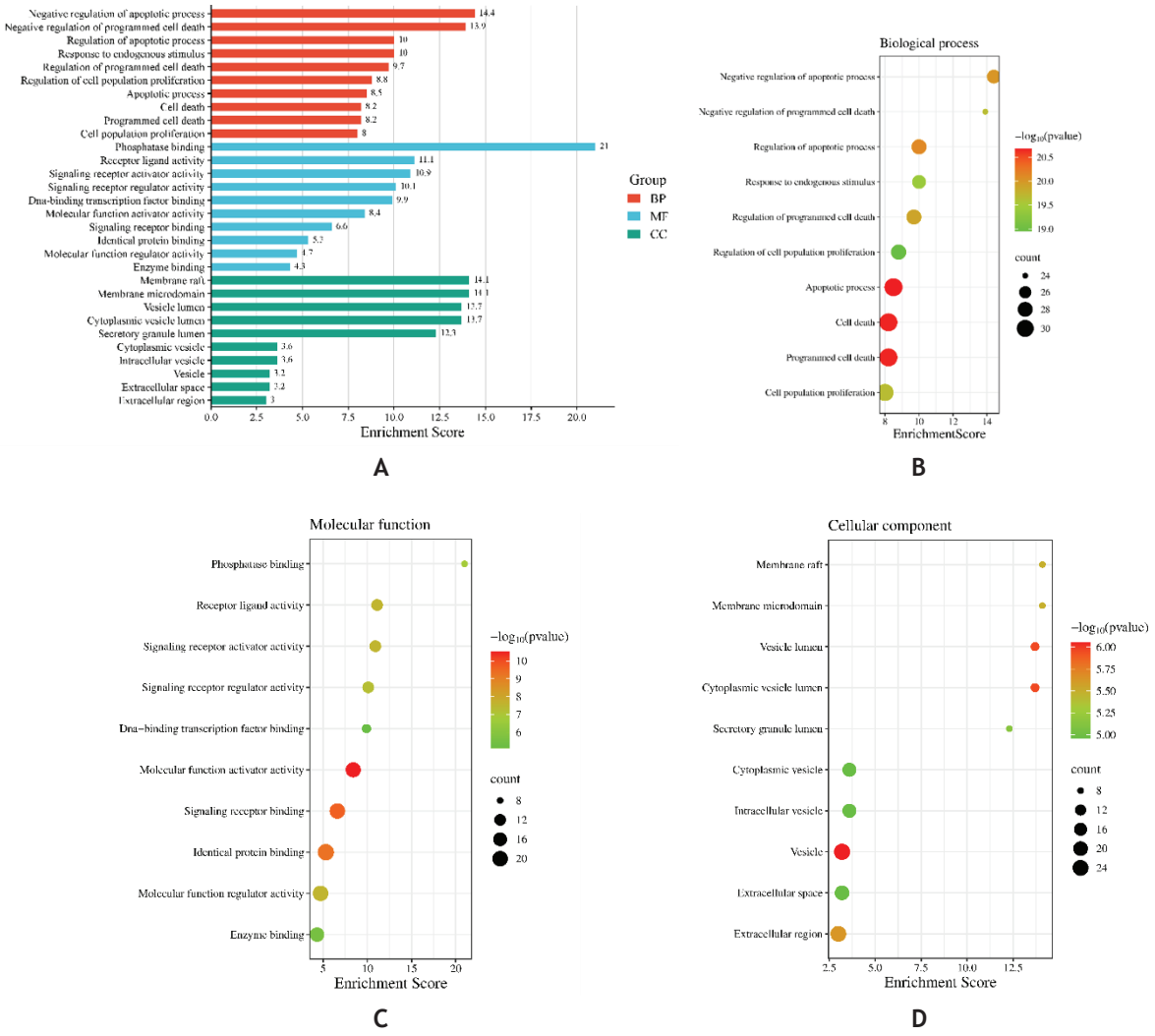


Figure 6. Gene Ontology (GO) analysis: A. GO bar chart of enrichment for biological processes, molecular functions, and cellular components; B. Enrichment bubble plot of the top 10 high-potential biological processes; C. Enrichment bubble plot of the top 10 high-potential molecular functions; and D. Enrichment bubble plot of the top 10 high-potential cellular components.

KEGG Pathway Analysis

Within the colorectal cancer-related signaling pathways, 11 target genes associated with andrographolide, 1,2,3-propanetriol–β-D-allopyranose (1:1), and 1,9-dideoxyforskolin were identified. These genes were EGF, AKT1, JUN, MYC, MAPK1, MAPK3, BAX, CCND1, BCL2, TP53, and CASP3.

The 11 target genes were associated with multiple colorectal cancer-related pathways, including the Wnt signaling pathway (hsa05210), MAPK signaling pathway (hsa04010), ErbB signaling pathway (hsa04012), PI3K signaling pathway (hsa04151), mTOR signaling pathway (hsa04150), apoptosis (hsa04210), and p53 signaling pathway (hsa04115).

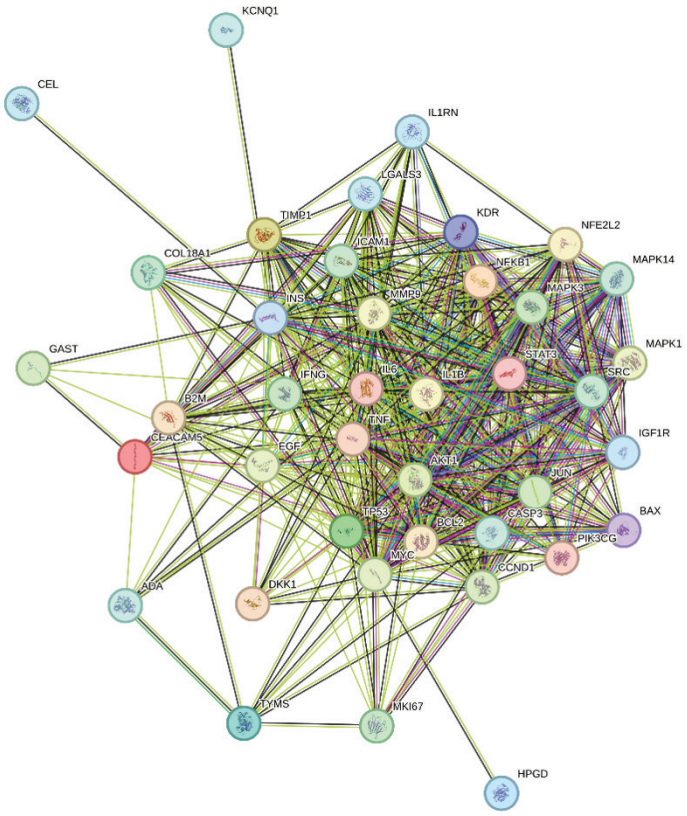


Figure 7. Interaction network of 40 core proteins from STRING database (40 nodes, 436 edges, PPI enrichment *p*-value: <1.0e-16.

The colorectal cancer pathway (hsa05210) contained 11 of 82 genes, with a strength of 1.82 and a false discovery rate (FDR) of 5.63E-16. The TNF signaling pathway contained 12 of 111 genes, with a strength of 1.73 and an FDR of 2.48E-16. The IL-17 signaling pathway contained 11 of 91 genes, with a strength of 1.77 and an FDR of 1.54E-15. The MAPK signaling pathway contained 15 of 286 genes, with a strength of 1.41 and an FDR of 2.71E-16. The apoptosis pathway contained 10 of 131 genes, with a strength of 1.58 and an FDR of 1.7E-12. The PI3K-Akt signaling pathway contained 14 of 349 genes, with a strength of 1.30 and an FDR of 8.67E-14.

Table 6. Results of the KEGG gene interaction analysis.

Pathway	Description	Count in Network	Strenght	False Discovery Rate
hsa05210	Colorectal cancer	11 of 82	1.82	5.63E-16
hsa04668	TNF signaling pathway	12 of 111	1.73	2.48E-16
hsa04657	IL-17 signaling pathway	11 of 91	1.77	1.54E-15
hsa04010	MAPK signaling pathway	15 of 286	1.41	2.71E-16
hsa04210	Apoptosis	10 of 131	1.58	1.7E-12
hsa04151	PI3K-Akt signaling pathway	14 of 349	1.3	8.67E-14

Indonesian Journal of Cancer Chemoprevention, October 2025
ISSN: 2088–0197
e-ISSN: 2355-8989

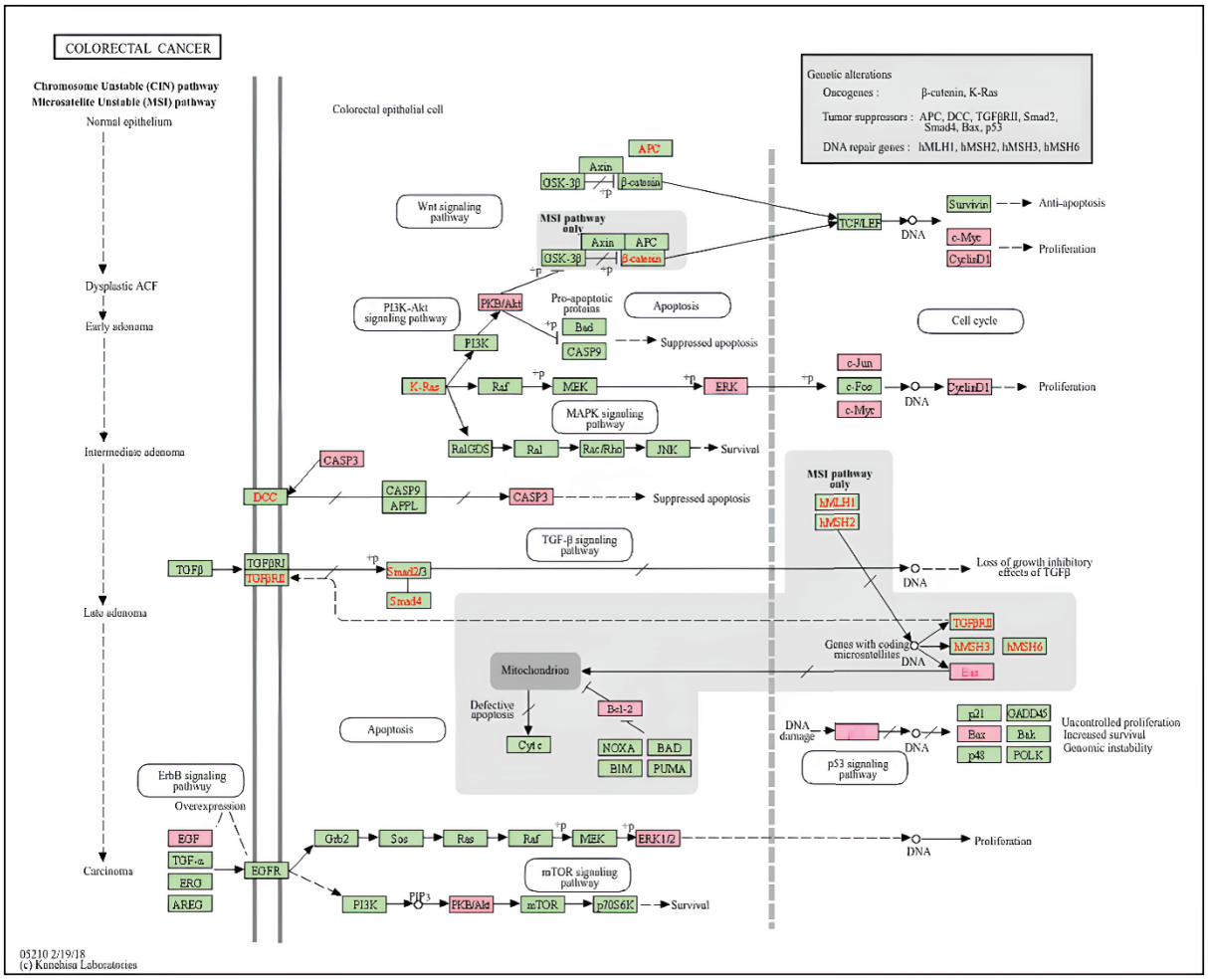


Figure 8. KEGG colorectal cancer pathway showing the localization of the 11 predicted target genes identified through network pharmacology analysis. Target genes are highlighted in pink.

DISCUSSION

Metabolite Profile and Putative Annotation The metabolite profiling of persimmon vinegar residue using UPLC-QToF-MS/MS demonstrated a complex chemical composition, as indicated by the multiple chromatographic peaks detected in the extract. The observed differences in retention time are consistent with the polarity-dependent separation characteristics of the C18 stationary phase and the gradient elution system used in the analysis (Hakim, *et al*., 2018). The use of high-resolution mass spectrometry and MS/MS fragmentation provided accurate mass measurements and characteristic fragmentation patterns that supported the putative annotation of the detected compounds (Lei, *et al*., 2023). Similar advantages of high-resolution UPLC-based approaches have also been reported in metabolomic studies (Lestari, *et al*., 2024).

Harmane was the most abundant annotated compound, accounting for 12.83% of the total peak area and showing a FitConf value of 92.3%. Harmane is a naturally occurring β-carboline alkaloid that has been reported in various plant-derived foods and fermented products and is there-

fore not specific to persimmon vinegar residue (Yang and Liu, 2024). Its detection in the present study, together with the other annotated metabolites, provides an indication of the chemical diversity present in persimmon vinegar residue.

Harmane has been reported to occur in plants, fermented foods, coffee, and tobacco (Piechowska, *et al*., 2019). Andrographolide is the principal diterpene lactone of Andrographis paniculata and is widely recognized as its major bioactive constituent (Zeng, *et al*., 2022). Meanwhile, 1,9-dideoxyforskolin belongs to the labdane diterpenoid family and has been reported as a natural constituent of Coleus forskohlii (syn. Plectranthus forskohlii).

The metabolite classes observed in this study are generally consistent with previous reports describing flavonoids, phenolic compounds, terpenoids, and organic acids in persimmon and persimmon-derived products (Mutiah, *et al*., 2026). However, the present study specifically focused on persimmon vinegar residue, which represents an underutilized fermentation by-product. Therefore, the observed metabolite profile provides additional information regarding its chemical composition and supports further investigation of its potential biological value.

Importantly, the metabolite annotations in the present study remain putative because authentic reference standards were not used for structural confirmation. Therefore, the detected compounds should not be interpreted as definitively identified metabolites. Further confirmation using authentic standards and complementary analytical approaches is required to establish the chemical identities of the detected compounds.

Predicted Drug-Likeness and Toxicity

The physicochemical prediction showed that 22 of the 25 evaluated compounds met the predefined criteria, whereas three compounds did not. Lipinski's Rule of Five was applied to estimate characteristics related to oral absorption based on molecular weight, log *P*, hydrogen bond donors, and hydrogen bond acceptors, together with torsional bonds and polar surface area. Compounds failing two or more of these criteria may have a higher likelihood of poor oral bioavailability (Praceka, *et al*., 2022).

The physicochemical parameters provide information regarding the characteristics that may influence the absorption and distribution of compounds. Log *P* reflects lipid solubility, while hydrogen bond donors and acceptors influence intermolecular interactions and potential absorption. Torsional bonds reflect molecular flexibility, whereas PSA represents the polar surface area of a molecule and may influence membrane permeability. Lower PSA values are generally associated with more favorable membrane permeability (Pramudiyawati, *et al*., 2024).

The toxicity prediction further showed that 21 compounds met the predefined toxicity criterion, whereas one compound, T-2 triol, did not. The LD_{50} values were classified according to toxicity classes described in Lu's Handbook of Toxicology, ranging from highly toxic categories to practically non- toxic categories (Mujtahid, 2024). In the present study, compounds with toxicity class ≥3 were considered to meet the predefined criterion.

These findings indicate that most of the evaluated compounds exhibited predicted physicochemical and toxicity characteristics considered acceptable within the computational screening criteria used in this study. However, these predictions should be interpreted as preliminary computational assessments rather than evidence of confirmed pharmacokinetic or safety profiles. Experimental studies are still required to establish actual absorption, distribution, metabolism, excretion, and toxicity characteristics.

Predicted Bioactivity of the Annotated Compounds

PASS Online analysis predicted eight compounds with Pa values greater than 0.5 for the

selected biological activities. Pa values greater than 0.7 indicate a higher predicted probability of activity, whereas values between 0.5 and 0.7 indicate moderate predicted activity (Hassan, *et al*., 2022). The predicted activities included antineoplastic, chemopreventive, and apoptosis agonist effects.

The predicted antineoplastic activity is relevant because antineoplastic agents act by inhibiting the growth and proliferation of cancer cells (Wicaksana, *et al*., 2024). Chemopreventive activity refers to the potential to suppress or reverse carcinogenic processes and prevent abnormal cells from progressing toward malignancy (Haryanti and Widiyastuti, 2017). Meanwhile, apoptosis agonists may promote programmed cell death, thereby contributing to the elimination of damaged or excessive cells (Fristiohady and Agustina, 2020).

Among the evaluated compounds, andrographolide showed the highest predicted Pa value for antineoplastic activity (0.949), as well as high predicted values for apoptosis agonist activity (0.909) and chemopreventive activity (0.640). It also showed a predicted Pa value of 0.538 for antineoplastic activity specific to colon cancer. 1,2,3-Propanetriol–β-D-allopyranose (1:1) and 1,9-dideoxyforskolin also demonstrated predicted antineoplastic, chemopreventive, and apoptosis agonist activities.

Network Pharmacology and Potential Molecular Mechanisms

The network pharmacology analysis identified 547 target proteins associated with the evaluated compounds, of which 40 overlapped with 162 colorectal cancer-related proteins obtained from DisGeNET. This overlap indicates that the evaluated compounds share a subset of predicted targets with proteins associated with colorectal cancer.

The 40 target proteins included CEACAM5, NFKB1, TIMP1, AKT1, TP53, VEGFA, TYMS, HPGD, KDR, BAX, STAT3, IL6, PIK3CG, TNF, DKK1, B2M, BCL2, NFE2L2, IL1B, MMP9, MAPK1, EGF, MYC, CCND1, GAST, JUN, MAPK3, IFNG, MKI67, ICAM1, SRC, MAPK14, CASP3, ADA, KCNQ1, LGALS3, CEL, IL1RN, IGF1R, and INS. These proteins are involved in processes related to cell proliferation, survival, inflammation, apoptosis, and other biological functions relevant to colorectal cancer.

Three compounds were associated with the identified target network: andrographolide, 1,2,3-propanetriol–β-D-allopyranose (1:1), and 1,9-dideoxyforskolin. The association of these compounds with the target network provides a basis for exploring their potential molecular relationships with colorectal cancer-related pathways.

The STRING analysis demonstrated 40 nodes and 436 edges, with a PPI enrichment p-value of $<1.0 \times 10^{-16}$. The high number of interactions and significant enrichment indicate that the identified proteins are functionally interconnectedrather than behaving as an entirely random group of proteins. Such interconnectedness may reflect their participation in coordinated biological processes (Baksh, *et al*., 2021).

Gene Ontology analysis showed enrichment across biological processes, molecular functions, and cellular components. Negative regulation of apoptotic processes showed the highest significance and involved 31 genes. Other enriched biological processes involved 27–31 genes. The enrichment of these processes is relevant to colorectal cancer because dysregulation of cell death and survival is an important characteristic of malignant progression.

The KEGG analysis further identified several pathways associated with the 11 key genes: EGF, AKT1, JUN, MYC, MAPK1, MAPK3, BAX, CCND1, BCL2, TP53, and CASP3. These genes were associated with the colorectal cancer, MAPK, ErbB, PI3K-Akt, mTOR, apoptosis, and p53 signaling pathways.

The Wnt signaling pathway is a major pathway involved in colorectal cancer development

because aberrant Wnt signaling can promote β-catenin accumulation and transcription of oncogenic genes such as MYC and CCND1. Both genes contribute to cellular proliferation and may inhibit apoptosis. Previous reports have indicated that 1,9-dideoxyforskolin may reduce β-catenin activity through activation of protein phosphatase 2A (PP2A), resulting in suppression of MYC expression. Andrographolide has also been reported to inhibit CCND1 transcription through down-regulation of β-catenin/TCF activity, potentially contributing to cell-cycle arrest and reduced cancer cell proliferation (O'Connor, *et al*., 2018).

The MAPK pathway is another important signaling pathway involved in colorectal cancer. Activation of the RAS–RAF–MEK–ERK cascade promotes phosphorylation of transcription factors such as c-Jun and c-Myc, which can enhance cancer cell proliferation and survival. Andrographolide has been reported to suppress ERK1/2 phosphorylation, resulting in reduced c-Jun activation and decreased cyclin D1 expression. In addition, 1,9-dideoxyforskolin has been reported to decrease MYC stability through PP2A activation, potentially attenuating MAPK-dependent proliferative signaling (Liu, *et al*., 2023).

The ErbB signaling pathway is associated with growth-factor-mediated cellular proliferation and differentiation. Binding of epidermal growth factor (EGF) to EGFR activates the RAS–RAF–MEK–ERK cascade, with MAPK1 and MAPK3 serving as important downstream effectors. These signaling components are frequently involved in colorectal cancer. Andrographolide has been reported to inhibit ERK1/2 phosphorylation, whereas 1,2,3-propanetriol–β-D-allopyranose (1:1) may influence EGF regulation, potentially affecting the initial activation of ErbB signaling (Li, *et al*., 2017). The PI3K/AKT pathway plays an important role in cancer cell growth and survival. AKT1 activation promotes protein synthesis and cellular proliferation and may contribute to resistance to apoptosis. Andrographolide has been proposed to reduce PI3K and AKT1 phosphorylation, thereby attenuating AKT-mediated pro-survival signaling. Inhibition of AKT1 may consequently suppress proliferation and increase cellular susceptibility to apoptosis (Han, *et al*., 2023).

The mTOR pathway is closely connected to PI3K/AKT signaling, with AKT1 acting as an upstream regulator of mTORC1. Activation of mTORC1 promotes protein synthesis and cell proliferation, while hyperactivation of mTOR is associated with tumor aggressiveness and therapeutic resistance. Therefore, suppression of AKT1 activity by andrographolide may indirectly reduce mTORC1 signaling and potentially inhibit cancer cell growth and survival (Manning and Toker, 2017).

The p53 pathway functions as an important cellular defense mechanism against DNA damage and malignant transformation. Activation of p53 can induce expression of BAX, which contributes to the intrinsic apoptotic pathway. Both andrographolide and 1,2,3-propanetriol–β-D-allopyranose (1:1) have been reported to enhance p53 activation, resulting in increased BAX expression and decreased BCL2 levels. An increased BAX/BCL2 ratio can facilitate cytochrome c release from mitochondria and promote apoptotic signaling (Tohkayomatee, *et al*., 2022).

The apoptosis pathway was also enriched in the network analysis. BCL2 and CASP3 are important regulators of cell survival and programmed cell death. Andrographolide has been reported to downregulate BCL2 expression and activate caspase-3, which functions as an executioner caspase in apoptosis. These mechanisms may contribute to enhanced apoptotic signaling and suppression of colorectal cancer progression (Satruhan and Patel, 2023).

Overall, the network pharmacology results indicate that the compounds and predicted targets may be associated with multiple signaling pathways involved in colorectal cancer. The simultaneous involvement of Wnt, MAPK, ErbB, PI3K-Akt,

mTOR, p53, and apoptosis pathways supports a potential multitarget mechanism. However, these associations are derived from database information and computational predictions and therefore should be considered hypotheses requiring experimental validation rather than confirmed molecular mechanisms.

Limitations and Future Perspectives

This study has several limitations. First, the network pharmacology analysis was conducted using publicly available databases and predictive algorithms, which may not fully capture the complex biological interactions involved in colorectal cancer. The number and identity of predicted targets may also depend on database coverage and the information available at the time of analysis.

Second, the metabolite annotations were based on accurate mass measurements and database matching without confirmation using authentic reference standards. Therefore, the compounds reported in this study should be considered putatively annotated rather than definitively identified.

Third, the proposed molecular mechanisms were derived from metabolomic profiling, bioactivity prediction, target prediction, PPI analysis, and pathway enrichment. These computational approaches provide hypotheses regarding possible biological mechanisms but do not directly demonstrate molecular interactions or biological effects in colorectal cancer models.

Future studies should therefore include molecular docking, molecular dynamics simulations, and *in vitro* or *in vivo* biological assays to validate the interactions between the putatively annotated metabolites and their predicted molecular targets. Experimental validation would also be necessary to confirm the biological activities and molecular mechanisms proposed in the present study.

Nevertheless, the present findings provide an initial scientific basis for further investigation of the bioactive compounds and potential biological value of *Diospyros kaki* L. vinegar residue as a potential source of anti-colorectal cancer agents.

CONCLUSION

The 96% ethanol extract of persimmon vinegar residue contains 25 putatively annotated metabolites, among which andrographolide, 1,9-dideoxyforskolin, and 1,2,3-propanetriol–β-D-allopyranose were identified as the key compounds associated with colorectal cancer–related target genes. These compounds exhibited favorable drug-likeness, acceptable predicted toxicity profiles, and potential biological activities. Network pharmacology analysis identified 11 key target genes, namely EGF, AKT1, JUN, MYC, MAPK1, MAPK3, BAX, CCND1, BCL2, TP53, and CASP3, which are involved in regulating cancer cell proliferation, apoptosis, and survival through multiple signaling pathways, including Wnt, MAPK, PI3K/Akt, mTOR, p53, and apoptosis. These findings address the research objective by characterizing the metabolite profile of persimmon vinegar residue and predicting its potential molecular mechanisms against colorectal cancer, thereby providing new insights into the valorization of persimmon vinegar fermentation residue as a potential source of natural anticancer agents. However, the metabolite annotations and therapeutic mechanisms remain based on computational prediction and require further experimental validation to confirm their biological activity and molecular interactions.

REFERENCES

Baksh, M., Iqbal, M.S., Yasmin, F., Suleman, S., Rasheed, M., Farooq, W., and Javed, T., 2021, Computational detection, analysis and

interpretations of genomic variants in human diseases-associated GENEMDM 2, *Biomedical Letters*, **7**(2), 141-154.

Bestari, S.A. and Albanna, W.A., 2025, Peran diet dalam mikrobiota saluran cerna pada pasien kanker kolon: Systematic Review, *Jurnal Kesehatan dan Pembangunan*, **15**(1), 242–250.

Bianchini, S., Bovio, F., Negri, S., Bisson, L., Piccinelli, A.L., Rastrelli, L., *et al.*, 2024, Methanolic extract of the nutritional plant (*Diospyros kaki* Thunb.) exhibits anticancer activity by inducing mitochondrial dysfunction in colorectal cancer cells, *Nutrients*, **16**(21), 3742.

Dalimunthe, N.A., 2021, Uji kualitatif analisis kandungan metamfetamin dari rambut pengguna sabu-sabu menggunakan metode kolom ekstraksi, *Jurnal Kimia Saintek dan Pendidikan*, **5**(1), 16–22.

Febriani, D.R. and Azizati, Z., 2018, Pembuatan Cuka Alami Buah Salak dan Pisang Kepok Beserta Kulitnya Teknik Fermentasi, *Walisongo Journal of Chemistry*, **1**(2), 72-77.

Fristiohady, A. and Agustina, I., 2020, Review artikel: Apoptosis pada kanker payudara, *Media Farmasi*, **16**(2), 130–140.

Hakim, A., Muti'ah, R., Aprinda, R., Suryadinata, A., and Maslakhah, F.N., 2018, Metabolite profiling bagian akar, batang, daun, dan biji Helianthus annuus L. menggunakan UPLC-MS, *Media Pharmaceutical Indonesiana*, **2**(2), 64–81.

Han, J., Tan, C., Pan, Y., Qu, C., Wang, Z., Wang, S., *et al.*, 2023, Andrographolide inhibits the proliferation and migration of vascular smooth muscle cells via PI3K/AKT signaling pathway and amino acid metabolism to prevent intimal hyperplasia, *European Journal of Pharmacology*, **959**, 176082.

Haryanti, S. and Widiyastuti, Y., 2017, Aktivitas sitotoksik pada sel MCF-7 dari tumbuhan Indonesia untuk pengobatan tradisional kanker payudara, Media Penelitian dan Pengembangan Kesehatan, **27**(4), 247–254.

Hassan, S.S.U., Abbas, S.Q., Ali, F., Ishaq, M., Bano, I., Hassan, M., *et al.*, 2022, A comprehensive *in silico* exploration of pharmacological properties, bioactivities, molecular docking, and anticancer potential of vieloplain F from *xylopia vielana* targeting B-Raf kinase, *Molecules*, **27**(3), 917.

Kemenkes, 2018, Keputusan Menteri Kesehatan Republik Indonesia Nomor HK.01.07/MENKES/406/2018 tentang Pedoman Nasional Pelayanan Kedokteran Tata Laksana Kanker Kolorektal, Jakarta: Kemenkes RI.

Kuncoro, H., Apriani, D.K., Naspiah, N. and Rahmadani, A., 2022, Isolasi, karakterisasi dan aktifitas radikal bebas DPPH senyawa metabolit sekunder dari fraksi etil asetat daun kokang (*Lepisanthes amoena* (Hassk) Leenh.), *Journal of Pharmacy and Science*, **5**(2), 1–10.

Lei, M., Wang, L., Olatunde, O.O.O., Singh, S., Ovatlarnporn, C., Basit, A., and Olatunji, O.J., 2023, UPLC–ESI–QTOF–MS profiling, antioxidant, antidiabetic, antibacterial, anti-inflammatory, antiproliferative activities and *in silico* molecular docking analysis of Barleria strigosa, *Chemical and Biological Technologies in Agriculture*, **10**, 73.

Lestari, P.E.D., Jannah, A.K.R.J., Hisan, H.K., Fitri, M.N. and Azharani, N.A., 2024, Analisis perbandingan HPLC dan teknik lain untuk deteksi antibiotik, *Termometer: Jurnal Ilmial Ilmu Kesehatan dan Kedokteran*, **2**(2), 01–11.

Li, Y., He, S., Tang, J., Ding, N., Chu, X., Cheng, L., 2017, Andrographolide Inhibits Inflammatory Cytokines Secretion in LPS-Stimulated RAW264.7 Cells through Suppression of NF- κ B/MAPK Signaling Pathway, *Evidence-Based Complementary and Alternative Medicine*, **2017**(1), 8248142.

Liigand, P., Kaupmees, K., Haav, K., Liigand, J., Leito, I., Girod, M., and Kruve, A., 2017, Think Negative: Finding the Best Electrospray Ionization/MS Mode for Your Analyte, *Analytical Chemistry*, **89**(11), 5665–5668.

Liu, Z., Jin, C., Zhang, Y., Jiang, Y., Wang, J., and Zheng, L., 2023, Identification of BRAF, CCND1,

and MYC mutations in a patient with multiple primary malignant tumors: a case report and review of the literature, *World Journal of Surgical Oncology,* **21**, 158.

Manning, B.D. and Toker, A., 2017, AKT/PKB signaling: navigating the network, *Cell*, **169**(3), 381–405.

Mutiah, R., Rachmawati, E., Taufik, I., Milliana, A., Ambar Sari, R., Rahmadani, N., Taufik, I., Milliana, A., Sari, R.A., Rahmadani, N., and Fitriyani, F., 2026, Metabolite Profiling and Network Pharmacology of Persimmon Vinegar (*Diospyros kaki*) Compounds, with *in silico* Validation for Non-Small Cell Lung Cancer Therapy, *Asian Pacific Journal of Cancer Prevention*, **27**(3), 955-965.

Mujtahid, I.F., Razak, R. and Najib, A., 2024, Studi *in silico* prediksi sifat fisikokimia dan toksisitas senyawa tectoquinone sebagai α-glukosidase inhibitor, *Makassar Natural Product Journal*, **2**(3), 215–221.

O'Connor, C.M., Perl, A., Leonard, D., Sangodkar, J., and Narla, G., 2018, Therapeutic targeting of PP2A, *The international Journal of Biochemistry & Cell Biology*, 96, 182-193.

Piechowska, P., Zawirska-Wojtasiak, R. and Mildner-Szkudlarz, S., 2019, Bioactive ß-carbolines in food: A review, *Nutrients*, **11**(4), 814.

Praceka, M.S., Yunita, E.N., Semesta, C.D., Putri, R.N., Mikdar, N.N., Sitinjak, E.N., *et al.*, 2022, Molecular docking and toxicity from temulawak rhizome (*Curcuma xanthorrhiza* Roxb.) against COX-2, *Indonesian Journal of Pharmaceutical Science and Technology*, **1**(1), 106–115.

Pramudiyawati, A., Putri, D.E., Nurfadilah, and Wilapangga, A., 2024, Skrining studi *in silico* potensi farmakokinetika dan toksisitas senyawa *6,10,14-trimetil-2-pentadekanon* dari ekstrak daun ekaliptus, *Indonesia Journal of Pharmaceutical Education*, **4**(1), 39-46.

Puspitasari, M.R. and Waluyo, A., 2021, Aplikasi teori katharine kolbaca pada kasus kanker kolon pasca laparatomi dengan musik, *Journal Medika Usada*, **4**(1), 1–6.

Satruhan and Patel, D.K., 2023, Andrographis paniculata (Burm. F.) Wall Ex. Nees: A Review on their active components and medicinal properties, *International Journal of Pharmacognosy and Life Science*, **4**(2), 111–119.

Tarigan, E.B., 2017, Beberapa komponen fisikokimia kakao fermentasi dan non fermentasi, *Jurnal Agroindustri Halal*, **3**(1), 048–062.

Tohkayomatee, R., Reabroi. S., Tungmunnithum, D., Parichatikanond, W. and Pinthong, D., 2022, Andrographolide exhibits anticancer activity against breast cancer cells (MCF-7 and MDA-MB-231 cells) through suppressing cell proliferation and inducing cell apoptosis via inactivation of ER-α receptor and PI3K/AKT/mTOR signaling, *Molecules*, **27**(11), 3544.

WHO, 2022, Cancer, Website, https://www.who.int, accessed on February 3, 2026.

Wicaksana, I.P.D.R., Astuti, N.M.W. and Siwananda, I.D.M., 2024, Analisis bibliometrik penelitian terkait potensi aktivitas antineoplastik isoflavon daun dadap serep, *Jurnal Ilmu Farmasi Nusantara*, **1**(1), 93–106.

Yang, I.F. and Liu, C., 2024, Combined Microbial Fermentation Converts Bioactive Compounds in Nitraria Tangutorum Bobrov Fruit and Displays its Antidiabetic Potential, *JSM Biotechnology and Biomedical Engineering*, **9**(1), 1093.

Zeng, B., Wei, A., Zhou, Q., Yuan, M., Lei, K., Liu, Y., *et al.*, 2022, Andrographolide: A review of its pharmacology, pharmacokinetics, toxicity, clinical trials, and pharmaceutical researches, P*hytotherapy Research*, **36**(1), 336–364.